Original Article: Open Access

VIBGYOR ePress

International Journal of
Metallurgy and Metal Physics

Effects of Nb and C Addition on Corrosion Resistance of Metal-Injection-Molded 440C Stainless Steel

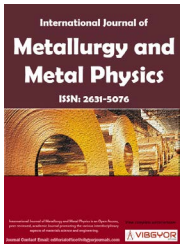

ISSN: 2631-5076

Yong Yu[1], Yimin Li[1,2*], Jia Lou[3], Hao He[2], Junfeng Wang[1] and Chen Liu[2]

[1]*State Key Laboratory of Powder Metallurgy, Central South University, China*

[2]*Research Centre for Materials Science and Engineering, Guangxi University of Science and Technology, China*

[3]*School of Materials Science and Engineering, Xiangtan University, China*

Abstract

The effects of Nb and C addition on the corrosion performance of metal-injection-molded 440C martensitic stainless steel were investigated. In addition to 440C and Nb440C samples, samples with different carbon contents were prepared from the Nb440C pre-alloyed powder mixed with graphite powders. The results show that Nb is uniformly distributed in the matrix in the form of carbides. This can reduce the activity of C in the matrix and inhibit grain growth. The corrosion resistance of all the samples was characterized by anodic polarization, electrochemical impedance spectroscopy, and double-loop electrochemical potentiokinetic reactivation analyses. The added Nb consumes C atoms in the matrix, allowing more Cr atoms to diffuse to the surface to form a passive film. As a result, resistance to pitting corrosion and intergranular corrosion is improved. However, increased carbon content negatively affects corrosion resistance.

Keywords

Metal injection molding, 440C stainless steel, Carbon content, Niobium, Corrosion resistance

Introduction

As a martensitic stainless steel, 440C stainless steel has high strength and hardness is widely used for transportation, machining, and in medical instruments [1-3]. However, stainless steel parts with small sizes and complex shapes are difficult to manufacture by traditional methods such as casting and machining. Hence, as a near-net-shape method, metal injection molding (MIM) is employed for the production of stainless steel parts [4].

In MIM, the carbon content fluctuates greatly due to the C/O and C/H reactions that occur during the sintering process [5-7]. These influence the mechanical properties and corrosion resistance of the product. High-C affinity elements can be added to reduce the activity of C in the matrix and so reduce the C fluctuation. Liu, et al. [8] reported that high-carbon affinity elements can reduce the diffusion rate of C in austenite. Nb is a typical high-carbon affinity element that can slow the diffusion

***Corresponding author:** *Yimin Li, State Key Laboratory of Powder Metallurgy, Central South University, 410083, Changsha; Research Centre for Materials Science and Engineering, Guangxi University of Science and Technology, 545006, China*

Accepted: August 03, 2019; **Published:** August 05, 2019

ISSN 2631-5076
9 772631 507005

Citation: Yu Y, Li Y, Lou J, He H, Wang J, et al. (2019) Effects of Nb and C Addition on Corrosion Resistance of Metal-Injection-Molded 440C Stainless Steel. Int J Metall Met Phys 4:035

of carbon and prevent decarburization. In addition, the formation of precipitate can refine the grain and help to increase the hardness and thermal stability of the steel [9-11]. At the same time, some researchers found that the addition of Nb in austenitic and ferritic stainless steels is beneficial as it stabilizes the passive film and enhances the corrosion resistance of the steel [12,13]. Dalmau, et al. [14] also found the same behavior in martensite. Jin, et al. [15] found that the interaction of Nb with C promotes the formation of a continuous film, which improves the corrosion resistance of low-alloy steel. These findings indicate that the addition of Nb has a positive effect on the corrosion resistance of stainless steel. While the addition of Nb and C into MIM of 4xx stainless steel is a popular topic [16-19], attention is generally focused on the densification and mechanical properties; the effects of Nb addition on the corrosion resistance of MIM440C stainless steel have rarely been reported. This paper reports the effects of Nb and C additions on the corrosion resistance of MIM440C stainless steel, with different carbon contents, and a preliminary analysis of the resistance mechanism.

Experimental Procedure

In this work, 440C and Nb440C pre-alloyed powders, supplied by Hunan Hengji Powder Technology Co. Ltd., were used. The chemical composition and particle size distributions of the powders are shown in Table 1. Graphite powders were added to the Nb440C stainless steel powders to obtain samples with different carbon contents: 0.15, 0.35, and 0.45 wt.%. The powders were mixed with the same wax-based binder, with a loading of 57 vt.%. The samples were prepared by injection molding after mixing and pelletizing. Solvent de-binding was performed by immersing the compacts in methylene chloride at 36 °C for 6 h. Then, thermal de-binding and pre-sintering were carried at 900 °C for 1 h in argon. Finally, the samples were sintered at 1340 °C for 2 h in a vacuum atmosphere of 1×10^{-1} Pa. The metallographies of the sintered samples were observed using a Leica DM2700M metallographic microscope. Phase analyses of the sintered samples were performed by X-ray diffraction (XRD) using a RINT2000 vertical goniometer at a scanning rate of 10°/min. The phase compositions were determined by comparing with the standard card. The elemental distributions of the samples were determined using an electron field emission JXA-8530F electron probe microanalyzer. The particle size of the raw material powder was detected by a Micro plus laser diffraction particle size analyzer. The powder carbon content was measured using a CS600 carbon-sulfur analyzer, and the oxygen content was measured using a TCH600 oxygen-nitrogen-hydrogen analyzer. Tensile strength was measured using an Inston3369 mechanical testing machine at a tensile rate of 2.0 mm/min.

Rectangular specimens with dimensions of 10 × 10 × 8 mm were cut from the sintered samples. After ultrasonic cleaning in alcohol, the 10 × 10 mm sides of the samples were exposed to the outside, while the other sides were connected to a copper wire. They were then embedded in epoxy resin, leaving an exposed working area of 10 × 10 mm. A CHI660E electrochemical workstation was used to characterize the corrosion properties of the materials. A conventional three-electrode cell was used, equipped with a saturated calomel electrode (SCE) as the reference electrode and a platinum plate as the counter electrode. Electrochemical impedance spectroscopy (EIS) tests were conducted in a 3.5 vol% NaCl solution. These were performed at the open-circuit potential, in the potentiostatic mode, with a voltage perturbation amplitude of 5 mV in the frequency range of 0.01-10^6 Hz. After this, the Tafel test was performed. The polarization curve scan started from -1 V to the anode, at a scan rate of 0.5 V/s, until the current density reached 500 mA/cm^2. Meanwhile, double-loop electrochemical potentiokinetic reactivation (DL-EPR) tests were conducted in a solution of 0.5 mol/L H_2SO_4 + 0.01 mol/L KSCN. The samples were kept immersed in the test solution for 0.5 h at the open-circuit potential. After obtaining a stable E_{corr}, the potential was raised by 0.1 mV/s. A reactivation scan followed the

Table 1: Chemical compositions and particle size distributions of powders.

Sample	Chemical compositions (wt.%)							Particle size (μm)		
	Cr	C	O	Si	Mn	Nb	Fe	D_{10}	D_{50}	D_{90}
Nb440C	15.50	0.95	0.06	0.75	0.71	1.74	Balance	4.76	13.00	27.50
440C	16.00	1.20	0.05	1.00	1.00	-	Balance	4.48	12.50	28.50

attainment of the predetermined potential (300 mV), returning to E_{corr}. The intersection of a straight line with the curve, generated by the application of a current of 10^{-4} A to each anodic polarization, was used as the pitting potential (E_b) of the samples. All the potentials were referred from the SCE. All the tests were performed at 20 °C.

Results and Discussion

Microstructure and mechanical properties

The carbon content, density, and average grain size of the sintered samples are shown in Table 2. With increasing initial carbon content, the carbon content of the sintered samples also increased.

Table 2: Carbon content, density, and average grain size of the samples.

Sample	Carbon content (wt%)		Relative density (%)	Average grain size (μm)
	Before sintering	After sintering		
440C	1.20	0.94	97.8	90.3
Nb440C	0.95	0.91	98.5	48.3
Nb440 + 0.15%C	1.10	1.02	97.5	52.1
Nb440 + 0.3%C	1.25	1.15	97.5	59.1
Nb440C + 0.45%C	1.40	1.33	97.5	65.3

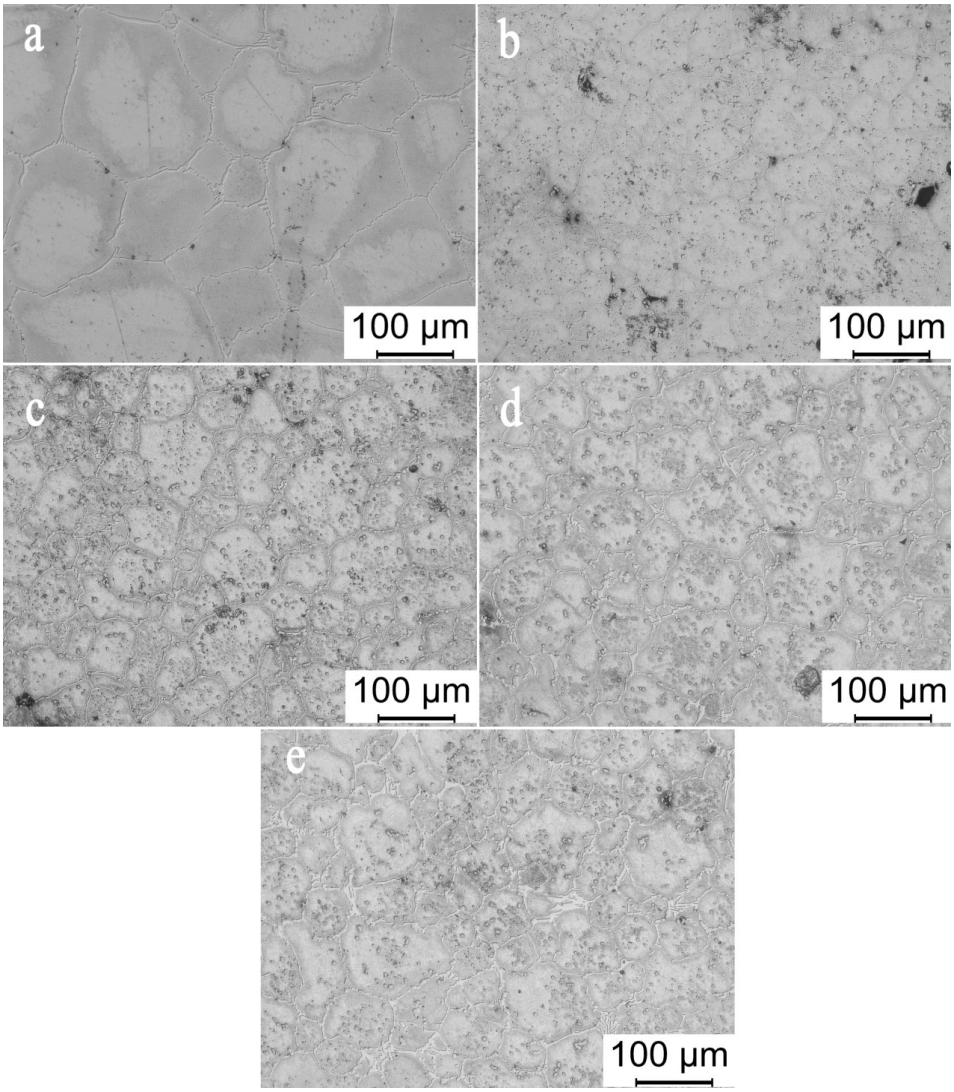

Figure 1: Microstructures of the samples: a) 440C; b) Nb440C; c) Nb440C + 0.15%C; d) Nb440C + 0.3%C and e) Nb440C + 0.45%C.

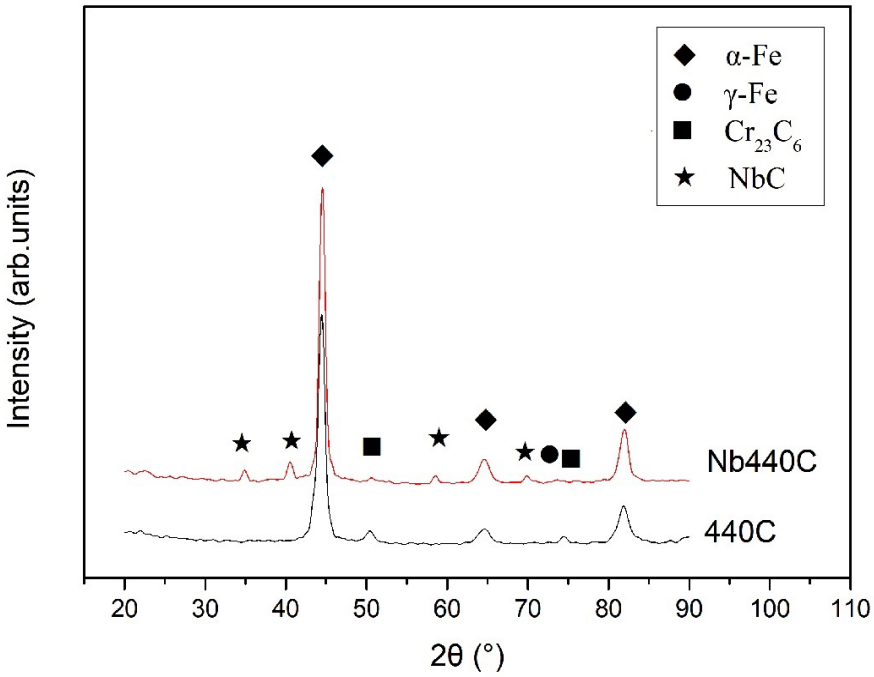

Figure 2: XRD results of Nb440C and 440C.

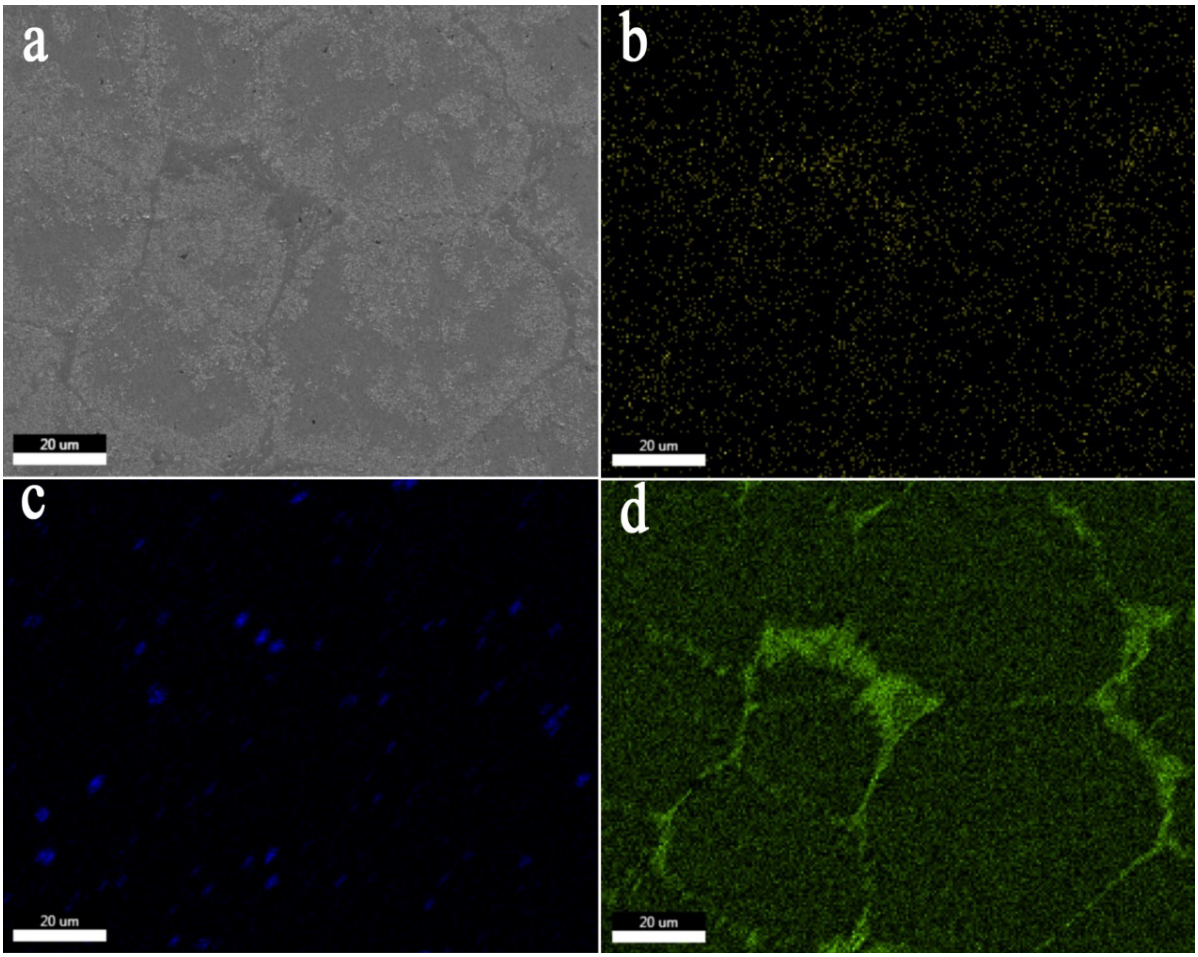

Figure 3: Elemental distributions of Nb440C: a) SEM; b) C; c) Nb; d) Cr.

Moreover, the samples with Nb exhibited a lower decarburization rate during sintering. Because Nb can form carbides with carbon and retard the diffusion of carbon, the carbon atoms become more difficult to shift to the surface of the sample for reaction with the atmosphere [8]. The densities of the samples reached much the same level, and densification was almost completed (> 97%), as shown in Table 2; therefore, the effects of density on corrosion resistance may be ignored.

The microstructures of the different samples are shown in Figure 1. The addition of Nb resulted in a smaller grain size and more carbide precipitation in the grain. The XRD results of Nb440C and 440C are shown in Figure 2. The addition of Nb did not change the main phase composition of the materials, yet NbC peaks were observed. The elemental distributions of Nb440C are shown in Figure 3. Most of the NbC precipitates were distributed on the grain boundaries. During sintering, these particles would inhibit grain growth. Consequently, Nb440C had a smaller grain size, as shown in Table 2.

The mechanical properties are shown in Figure 4. The hardness was similar for all samples. However, the tensile strength was significantly improved with the addition of Nb. On the other hand, with increasing carbon content in Nb440C, the tensile strength decreased remarkably. The higher the carbon content, the more NbC second phases precipitated in the matrix. The NbC precipitates are the origins of cracks during deformation and so decrease the tensile strength of the material. Moreover, a smaller grain size of Nb440C can promote strength.

Pitting resistance

The anodic polarization curves of the different samples in the 3.5 vol% NaCl solution are shown in Figure 5. The curves have no obvious passivation zone, and the corrosion current density increases rapidly after the dynamic potential sweep through the corrosion potential. Table 3 presents the parameters of the anodic polarization curves of the different samples; Nb440C had a lower I_{corr} and higher E_{corr} and E_b than the other samples. When E_b is higher, pitting resistance improves. Thus, the results show that Nb440C has good corrosion resistance. With increasing carbon content, the I_{corr} of the samples increased, while the E_{corr} and E_b decreased and corrosion resistance was reduced. Table 2 shows that the carbon content of 440C and Nb440C are similar; hence, the effects of the carbon content on corrosion resistance may be ignored. It is evident, therefore, that the addition of Nb improves the pitting resistance of 440C stainless steel.

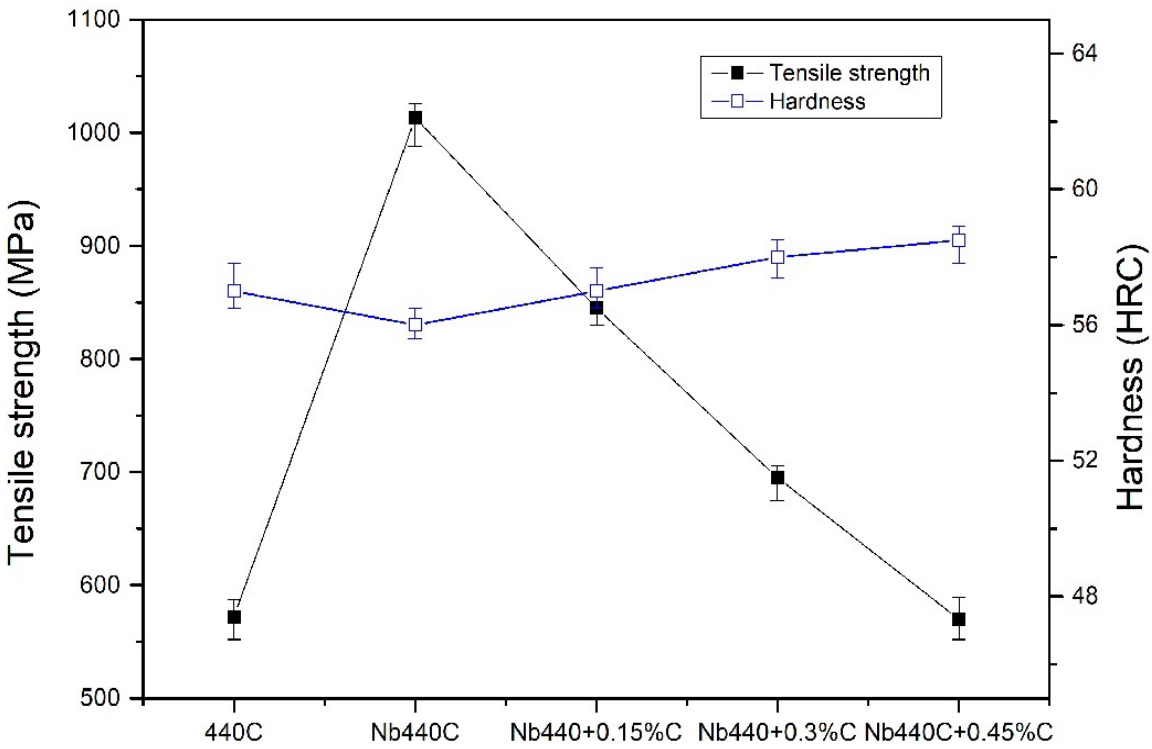

Figure 4: Mechanical properties of the samples.

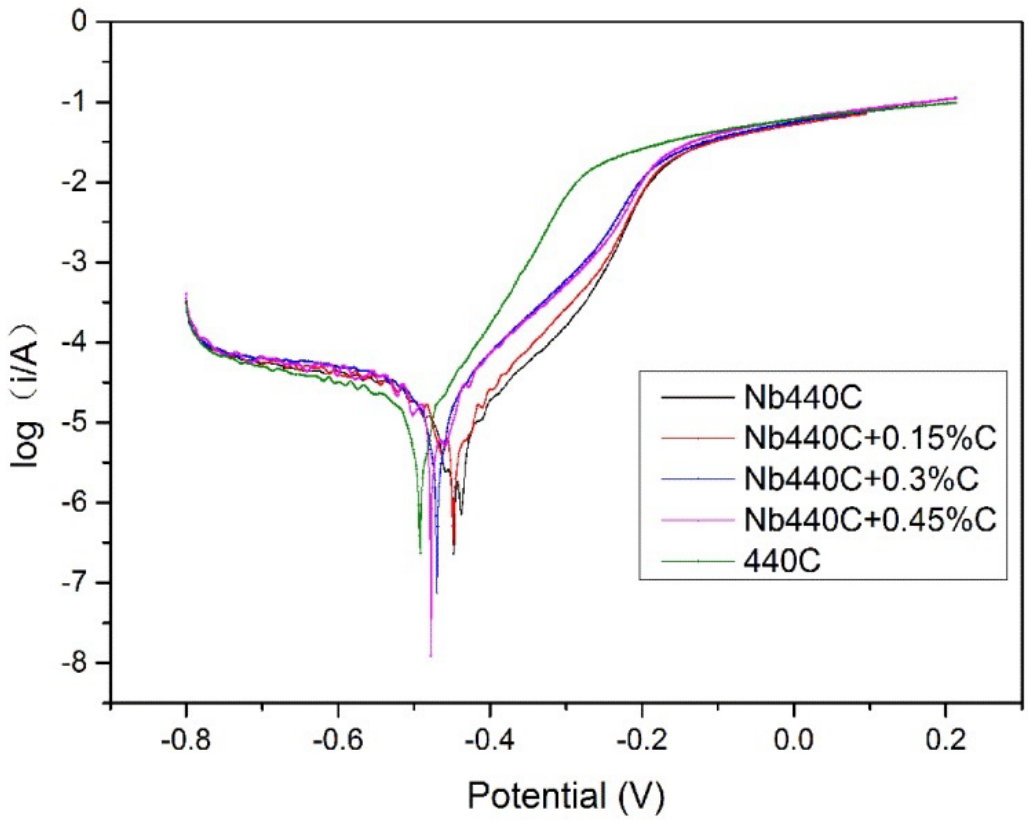

Figure 5: Anodic polarization curves of the samples in 3.5 vol% NaCl solution.

Table 3: Results from the anodic polarization curves of the samples.

Sample	E_{corr} (V)	I_{corr} (A/cm²)	E_b (V)
440C	-0.492	4.288×10^{-5}	-0.416
Nb440C	-0.448	8.995×10^{-6}	-0.321
Nb440C + 0.15%C	-0.448	2.207×10^{-5}	-0.341
Nb440C + 0.3%C	-0.47	2.99×10^{-5}	-0.386
Nb440C + 0.45%C	-0.478	4.25×10^{-5}	-0.389

Figure 6 presents the impedance spectra in the form of Nyquist curves of the samples in the 3.5 vol% NaCl solution. Table 4 shows the EIS data of the samples. It can be seen that the Nb440C sample has a larger diameter arc than the 440C sample. This indicates that Nb440C has a larger charge transfer resistance, but this gradually decreases with increasing carbon content. Thus, the addition of Nb increases corrosion resistance. However, addition of carbon has a negative effect on resistance.

The pitting resistance of stainless steel is mainly influenced by a passive film, formed by Cr_2O_3, with a thickness of ten to hundreds of nanometers [20]. Some research has shown that Nb is present,

Table 4: EIS curve data of the samples.

Sample	Surface resistance (Ω/cm²)
440C	6.62×10^2
Nb440C	1.57×10^3
Nb440C + 0.15%C	1.21×10^3
Nb440C + 0.3%C	1.09×10^3
Nb440C + 0.45%C	1.01×10^3

primarily in the form of carbonitrides, in the matrix [21]. However, the nitrogen content of 440C steel is extremely low, and it mainly exists in the form of carbides. The presence of Nb-containing carbides is evident in Figure 2 and Figure 3. The formation of these carbides consumes the C atoms in the stainless steel and thus reduces the Cr content held in carbides. In this way, more Cr can be used to form the passive film, which in turn improves the pitting resistance. Additional carbon content may offset this tendency.

Resistance to intergranular corrosion

Figure 7 shows the DL-EPR curves of different samples in the 0.5 mol/L H_2SO_4 + 0.01 mol/L KSCN solution. The reactivation current density (I_r) and

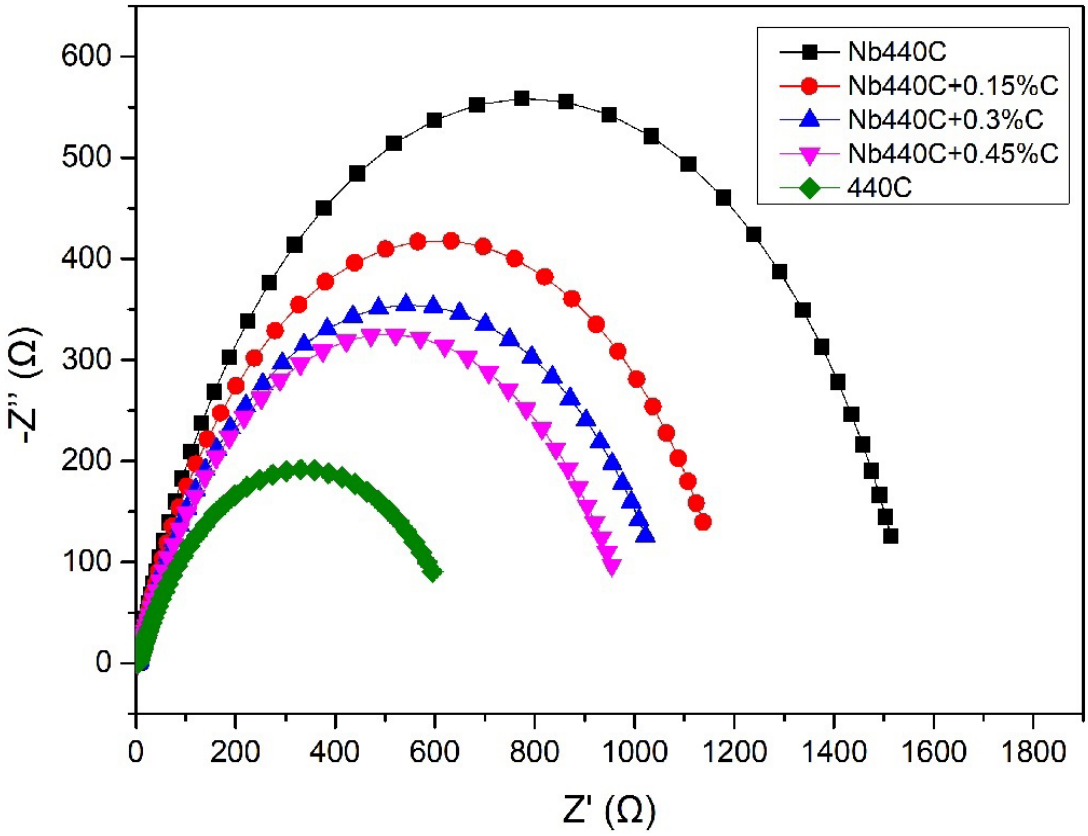

Figure 6: Nyquist curves of the samples in 3.5 vol% NaCl solution.

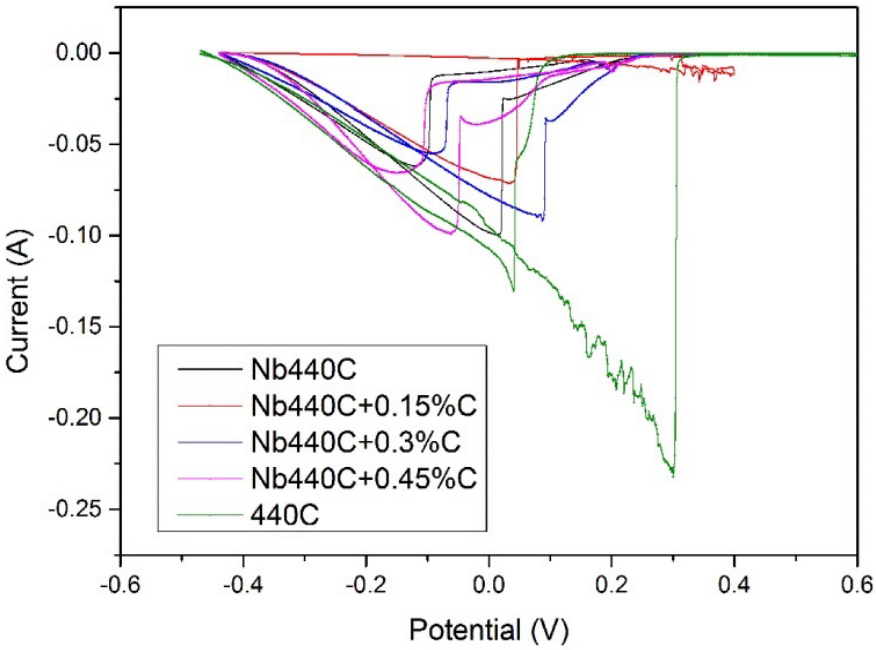

Figure 7: DL-EPR curves of samples in 0.5 mol/L H_2SO_4 + 0.01 mol/L KSCN solution.

activation current density (I_a) were measured and their ratio $R_a(\%) = I_r/I_a$ was calculated, as shown in Table 5. The value of R_a represents the degree of sensitization to intergranular corrosion of the specimens. The R_a value was found to increase with increasing carbon content. This indicates that increasing the carbon content reduces resistance to intergranular corrosion in Nb440C stainless steel.

Table 5: R_a values of the samples.

Sample	R_a (%)
440C	63.3
Nb440C	59.9
Nb440C + 0.15%C	61.0
Nb440C + 0.3%C	62.1
Nb440C + 0.45%C	62.9

Susceptibility to intergranular corrosion of stainless steels is related to the depletion of chromium along the grain boundaries as a result of precipitation of chromium carbides or other chromium-rich phases [22]. Nb is a strong carbide stabilizing element, the formation tendency of NbC is larger than that of $Cr_{23}C_6$. Thus, the carbon atoms preferentially form NbC with Nb. As a result, the amount of chromium consumed by the formation of $Cr_{23}C_6$ near the grain boundary is also reduced. At the same time, Nb440C has a smaller grain size than the other samples, as shown in Figure 1. The smaller grain boundary size means that the grain boundary area is greatly increased. To form an equal amount of $Cr_{23}C_6$, chromium may be drawn from a larger area, resulting in less chromium atoms being consumed near the grain boundary [23]. Therefore, the addition of Nb to MIM440C stainless steel can improve resistance to intergranular corrosion. However, increased carbon content has the opposite effect.

Conclusion

1. In MIM Nb440C stainless steel, NbC precipitates are formed. Most NbC precipitates are distributed on the grain boundaries, which inhibits grain growth.
2. The formation of NbC precipitates in stainless steel consumes carbon atoms, and reduces the tendency to form carbides with chromium. Thus, the pitting resistance of the 440C steel is improved. However, carbon content has the opposite effect.
3. NbC reduces the degree of chromium depletion near the grain boundary and refines the grains. It also reduces R_a and improves resistance to intergranular corrosion of 440C stainless steel. On the other hand, increase in carbon content will increase R_a and reduce resistance to intergranular corrosion.

Acknowledgement

The authors acknowledge support from the Guangxi Provincial Natural Science Foundation (Grant No. 2017GXNSFBA198187), the Liuzhou Science and Technology Plan Project (Grant No. 2018DH10505), and the China Postdoctoral Science Foundation (Grant No. 2018M632978).

References

1. R Bush, J Gill, J Teakell (2016) Heat treatment optimization and fabrication of a 440C stainless steel knife. JOM 68: 3167-3173.
2. SH Salleh, MN Derman, MZ Omar, J Syarif, S Abdullah (2013) Microstructure and properties of heat-treated 440C martensitic stainless steel. Defect and Diffusion Forum 335: 105-110.
3. S Thamizhmanii, R Ahmad, S Hasan (2011) Performance of CBN and PCBN tools on the machining of hard AISI 440C martensitic stainless steel. Advanced Materials Research 264-265: 1137-1147.
4. HZ Ye, XY Liu, HP Hong (2008) Fabrication of metal matrix composites by metal injection molding-A review. Journal of Materials Processing Tech 200: 12-24.
5. AJ Coleman, K Murray, M Keams, TA Tingskog, B Sanford, et al. (2013) Properties of MIM AISI 420 via pre-alloyed and master alloy route. Powder Metallurgy Particulate Material.
6. WSW Harun, K Toda, T Osada, H Kang, F Tsumori, et al. (2012) Effect of MIM processing parameters on the properties of 440C stainless steel. J Jpn Soc Powder Powder Metallurgy 59: 264-271.
7. O Karabelchtchikova (2007) Fundamentals of mass transfer in gas carburizing. Worcester Polytechnic Institute, USA.
8. P Liu, WW Xing, X Cheng, XQ Chen (2014) Effects of dilute substitutional solutes on interstitial carbon in α-Fe: Interactions and associated carbon diffusion from first-principles calculations. Phys Rev B 90: 1-13.
9. KT Huang, SH Chang, PC Hsieh (2017) Microstructure, mechanical properties and corrosion behavior of NbC modified AISI 440C stainless steel by vacuum sintering and heat treatments. Journal of Alloys and Compounds 712: 760-767.
10. H Kotan (2018) Thermal stability, phase transformation and hardness of mechanically alloyed nanocrystalline Fe-18Cr-8Ni stainless steel with Zr and Y_2O_3 additions. Journal of Alloys and Compounds 749: 948-954.
11. H Kotan (2015) Microstructural evolution of 316L

stainless steels with yttrium addition after mechanical milling and heat treatment. Materials Science and Engineering: A 647: 136-143.

12. AS Hamdy, E EL-Shenawy, T Elbitar (2006) Electrochemical impedance spectroscopy study of the corrosion behavior of some niobium bearing stainless steels in 3.5% NaCl. Int J Electrochem Sci 1: 171-180.
13. M Seo, G Hultquist, C Leygraf, N Sato (1986) The influence of minor alloying elements (Nb, Ti and Cu) on the corrosion resistivity of ferritic stainless steel in sulfuric acid solution. Corrosion Science 26: 949-960.
14. A Dalmau, C Richard, AI Munoz (2018) Degradation mechanisms in martensitic stainless steels: Wear, corrosion and tribocorrosion appraisal. Tribology International 121: 167-179.
15. YF Jin, T Zhang, QY Zang, YT Yang (2019) Behavior of Nb influence on structure and properties of 30Cr13 cast martensitic stainless steel. Journal of Iron and Steel Research International 26: 462-471.
16. XZ Huang, SY Chen, X Zhang, YT Yang (2014) Effect of heat treatment processes on microstructure and mechanical properties of Nb-Ti-Stabilized 430 stainless steel plate. Advanced Materials Research 887-888: 240-247.
17. YU Shengwang, K You, X Liu, Y Zhang, Z Wang, et al. (2016) Surface Nb-alloying on 0.4C-13Cr stainless steel: Microstructure and tribological behavior. Surface Review and Letters 23: 7-11.
18. A Kumar, RK Gupta, MK Karthikeyan, PR Kumar, PP Sinha (2012) Comparative study on tempering response of martensitic grade AISI-420 stainless steels with varying carbon content. Materials Science Forum 710: 489-494.
19. CF An, H He, YM Li (2018) Effect of carbon and Nb on sintering densification and mechanical properties of MIM 420 stainless steel. Journal of Guanxi Unversity of Science and Technology 29: 63-69.
20. MP Ryan, DE Williams, RJ Chater, BM Hutton, DS McPhail (2002) Why stainless steel corrodes. Nature 415: 770-774.
21. PJ Jorgensen, JH Westbrook (2010) Role of solute segregation at grain boundaries during final-stage sintering of alumina. Journal of the American Ceramic Society 47: 332-338.
22. LG Zheng, XQ Hu, XH Kang, DZ Li (2013) Evaluation of the susceptibility to intergranular corrosion for a novel Cr-Mn-N austenitic stainless steel using DL-EPR. Advanced Materials Research 631-632: 192-197.
23. J Armijo (1968) Intergranular corrosion of nonsensitized austenitic stainless steels. Corrosion 24: 24-30.

ISSN 2631-5076
9 772631 507005